

Geometry Optimisation of a Pneumatic Extension Nozzle for Sample Introduction in Atomic Emission Spectrometry (AES)

S. Groom*, P. Walzel

University of Dortmund
Department of Chemical Process Engineering
Chair of Mechanical Process Engineering
[*s.groom@ct.uni-dortmund.de](mailto:s.groom@ct.uni-dortmund.de)

Abstract

Atomic emission spectrometry (AES) is a commonly applied method in analysing trace elements. In AES pneumatic nebulizers are mostly used for sample introduction. Only droplets with diameters smaller than $10\text{ }\mu\text{m}$ are valid for this analytical method, the applied nebulizer must generate a comparatively fine aerosol. The nozzle diameter d of usually in AES applied nebulizers vary in a range of $100\text{ }\mu\text{m} < d < 250\text{ }\mu\text{m}$. The introduction of aerosols with an increased mass fraction of droplets with a useable diameters $D < 10\text{ }\mu\text{m}$ leads to an enhancement of the analytical signal. Thus, a higher signal resolution is given by an improved atomizer resulting in lower detection limit.

A comparison of different frequently used nebulizers in AES with a prototype of the proposed Pneumatic Extension Nozzle PEN was conducted in a prior work [1]. This investigation has indicated that at the entire range of operating conditions the PEN always produces a finer aerosol with smaller Sauter mean diameters D_{32} and larger mass fractions of desired droplets at given outlet diameters. At special operating conditions the PEN generates a nearly 3.5 times larger mass fraction of droplets with $D < 10\text{ }\mu\text{m}$ as a Concentric Pneumatic Nebulizer CPN, which is commonly applied in AES.

An enlarged model with $d = 2\text{ mm}$ was used in order to characterize the influence of special geometrical dimension on the Sauter mean diameter D_{32} . Thereby, the distance between the capillary and the orifice and also the curvature radius r of the gas orifice outlet is in special interest. The geometry of the PEN should be optimized according to the results as presented here.

In case of the PEN an optimum distance between the capillary and the orifice was found at $a = d_o/4$. The smallest D_{32} were achieved using a sharp-edged orifice. The transition of disintegration regimes could be observed by means of a high-speed CCD-camera and an enlarged transparent model of the PEN. The disintegration regime atomization is characterised by the formation of several comparatively thin ligaments. Their break-up leads to a strong decrease of the mean drop size of the aerosol. The transition between the disintegration regimes under different conditions are characterised in a diagram. The geometrical dimensions of PEN have a substantially influence on the disintegration regime at given operating conditions.

1. Introduction

1.1 Sample introduction in Atomic Emission Spectrometry AES

Atom emission spectrometry is one of the most frequent methods for trace element analysis. The sample is introduced in a high temperature plasma by the means of pneumatic nebulizers usually. Inside the plasma the sample atoms are excited due to the high temperature. Thereby, light with a characteristic wave length spectrum is emitted from the atoms. This spectrum can be assigned to single substances. In order to prevent serious disturbances of the analytical signal the sample has to be evaporated completely. However diameters larger than $10\text{ }\mu\text{m}$ are not completely evaporated during the short residence time in the spectroscopical source. Using commonly nebulizers only 10 to 20 percent of the aerosol mass has a desired droplet diameters with $D < 10\text{ }\mu\text{m}$. Therefore, larger droplets must be removed from the aerosol before being introduced into the excitation source. Therefore a separation chamber is switched between the nebulizer and the excitation source. Finally, only 1 to 2 percent of the sprayed sample mass reaches the spectroscopical source due to the small part of suitable droplets produced by the nebulizer and due to the insufficient separation efficiency of the precipitation chambers for smaller droplets.

1.2 Comparative investigation of different pneumatic nebulizers

The standard nebulizer used in AES is shown in Fig. 1a. This concentric pneumatic nebulizer (CPN) is applied in almost 90 percent of all AES devices [2]. The liquid sample is fed to a fine capillary of $d_c = 250\text{ }\mu\text{m}$ in diameter at the outlet position. The gas flows coaxial to the liquid through an annular slot with an average width of $20\text{ }\mu\text{m}$ at the outlet position. This nebulizer was compared with a Pneumatic Extension Nozzle (PEN) which is quite new for sample introduction in AES. A miniaturized prototype of the PEN is shown in Fig. 1b.

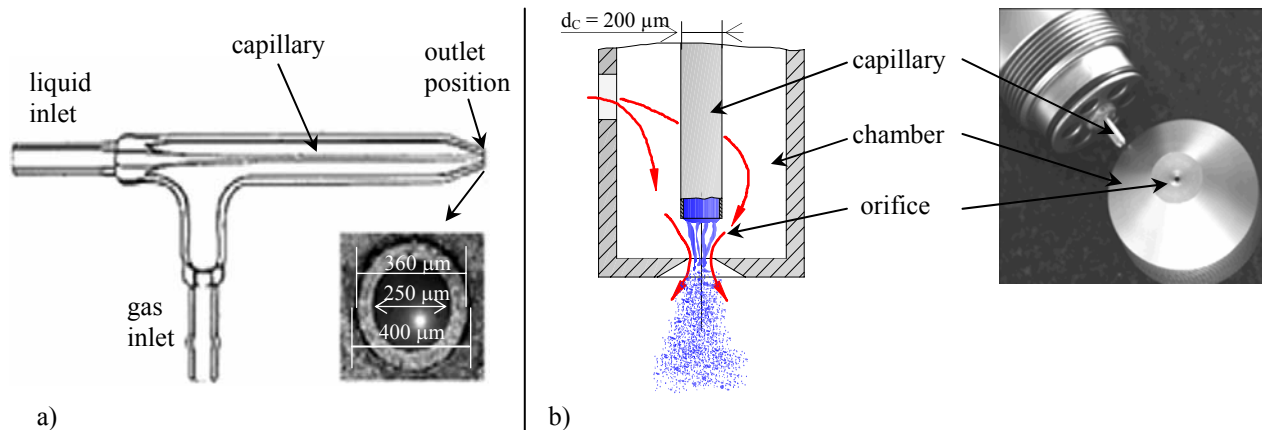


Fig. 1: a) Concentric Pneumatic Nebulizer (CPN) commonly used in AES; b) cross section and picture of the prototype of the Pneumatic Extension Nozzle (PEN)

Inside the chamber of the PEN, which is passed by the gas, the liquid discharges from a capillary with $d_c = 200\text{ }\mu\text{m}$. At comparatively small gas pressures a liquid jet is formed. The gas combined with the jet passes the orifice with a diameter of $d_o = 200\text{ }\mu\text{m}$. The jet is constricted due to the aerodynamic forces of the gas and the gas pressure gradient at the orifice. Outside the chamber the jet disintegrates into ligaments first and finally form droplets due to the Rayleigh mechanism. This, so called laminar jet disintegration, is characterised by a narrow droplet size distribution. At higher gas pressures asymmetric aerodynamic waves are visible

on the jet surface. A further rise of gas pressure results in a turbulent, i.e. more chaotic, atomization process. Then smaller droplets are produced, but the size spectrum of the droplets becomes wider. A similar method has been already applied in 1966 by Walz [3] for the production of rock and glass wool. In order to generate approximately monosized droplets Gañán-Calvo and Barrero [4] examined laminar microjets disintegrated by the Rayleigh mechanism. The authors applied a nozzle similar to the PEN however within the laminar flow range of the gas.

Within this investigation both nebulizers were operated at comparable conditions. The comparability of the measurements of different nozzles requires the use of dimensionless characteristic numbers. The Gas-Laplace-number $\Delta p_g^* = \Delta p_g d / \sigma_l$ and the liquid to gas mass ratio $\mu = \dot{m}_l / \dot{m}_g$ were varied during the investigation in a range of $500 \leq \Delta p_g^* \leq 700$ and $0.5 \leq \mu \leq 3.0$. The Ohnesorge-number was maintained at $On = \eta_l / (d \cdot \sigma_l \cdot \rho_l) = 0.008$. A result of this investigation is shown in Fig. 2.

Only droplets with diameters smaller than $10 \mu\text{m}$ are suitable for the AES. Therefore, the aerosol should consist the largest possible mass fraction of these droplets. Fig. 2 shows the cumulative droplet size distributions of the PEN and CPN at $\Delta p_g^* = 600$, $\mu = 0.5$ and $On_l = 0.008$. A Laser-Phase-Doppler-Analyser (LPDA) was used for the measurement of drop sizes.

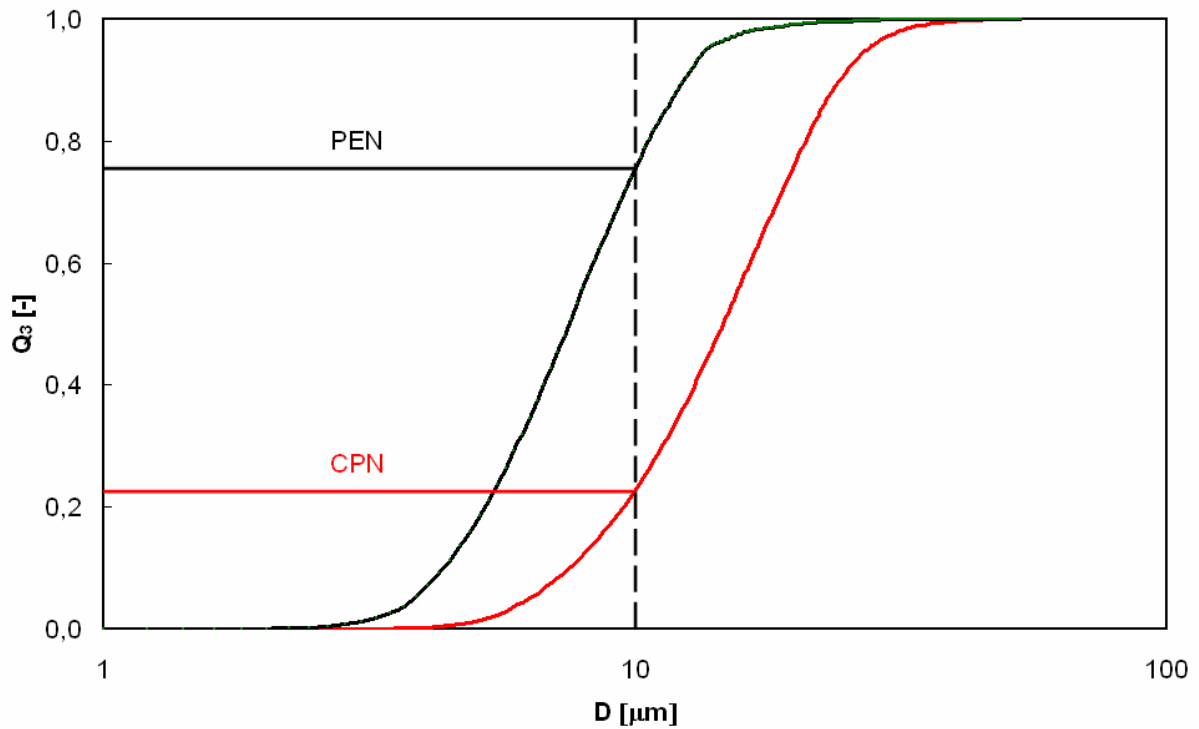


Fig. 2: Cumulative drop mass distribution Q_3 for the two nebulizers at $\Delta p_g^* = 600$ and $\mu = 0.5$, LPDA-reading

The CPN generates an aerosol mass fraction of droplets with $D < 10 \mu\text{m}$ of approximately 23 %. The Aerosol from PEN contains approximately 78 mass percent of suitable droplets. Thus, the PEN forms a nearly 3.5 times larger mass fraction of useable droplets as the CPN, most commonly applied in AES.

2. Variation in geometry

Further enhancement of the mass fraction should be promoted by a geometrical optimization of PEN. Current literature gives no sufficient knowledge about the effect of geometrical dimensions of PEN on the resulting aerosol. The distance a between the capillary and the orifice proved to be an important geometric parameter, which affected the aerosol generation. Therefore, a fundamental study about the geometrical effects was accomplished by an enlarged model with $d_C = d_O = 2$ mm. The distance a , as well as the radius r of the orifice outline, were varied during this investigation. The Sauter mean diameter D_{32} was measured applying a Laser Diffraction Spectrometer LDS. Fig. 3 shows the examined orifice geometries with different inlet radii r at the gas orifice. The Gas-Laplace-number Δp_g^* was varied in a wide range of $50 \leq \Delta p_g^* \leq 1000$.

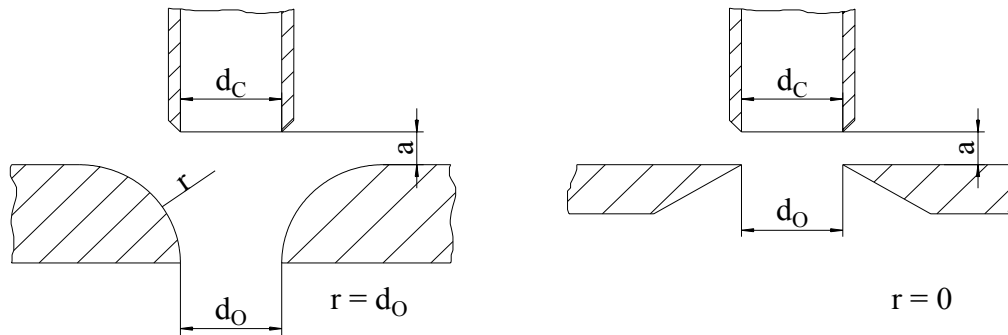


Fig. 3: Tested orifice geometries a) rounded orifice with $r = d_O$; b) sharp-edged orifice with $r = 0$, distance a was also varied

3. Experiments

In Fig. 4 the Sauter mean diameter D_{32} is plotted versus the liquid to air mass ratio μ at a Gas-Laplace-number of $\Delta p_g^* = 500$. The ratio d_O/d_C was maintained at a value of 1.0. The applied PEN has a sharp-edged gas orifice with an outline radius $r = 0$. A Laser-diffraction-Spectrometer was used for the measurement of the drop size distribution. The measurements are started with a distance $a = d_O = 2$ mm. Then the distance a was halved step by step. The reduction of the distance from $a = d_O$ to $a = d_O/2$ shows no effect on the Sauter mean diameter D_{32} . At a distance of $a = d_O/4$ the smallest Sauter mean diameter D_{32} were achieved during this first test. At this distance the cross section areas of the orifice and the cylindrical part between the capillary and the orifice become equal. Otherwise a further decreasing of $a = d_O/8$ again leads to an increasing of the Sauter mean diameter D_{32} .

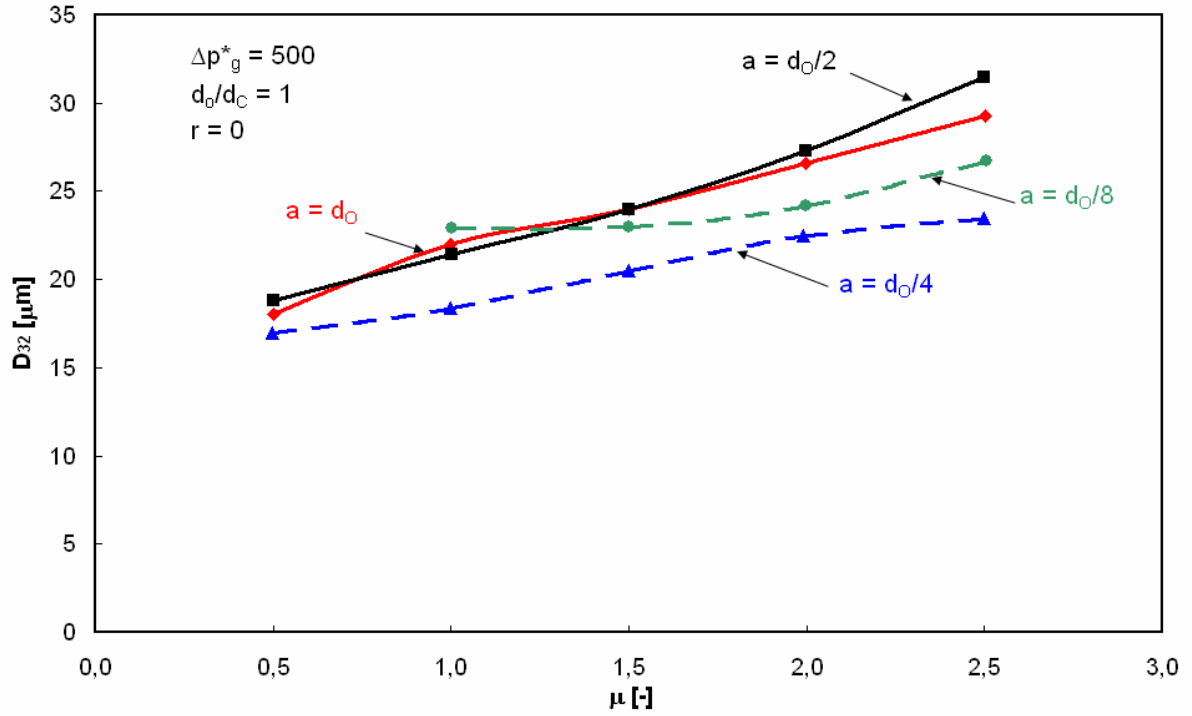


Fig. 4: Sauter mean diameter D_{32} versus liquid to air mass flow ratio μ at $\Delta p_g^* = 500$ for $d_O/d_C = 1$ and $r = 0$ (sharp-edged orifice). The distance a between orifice and capillary was varied

Fig. 5 illustrates the Sauter mean diameter D_{32} in dependence on the distance a . Therefore, the Gas-Laplace-number was varied in a range of $200 \leq \Delta p_g^* \leq 800$ at a constant liquid to air mass ratio of $\mu = 1.0$.

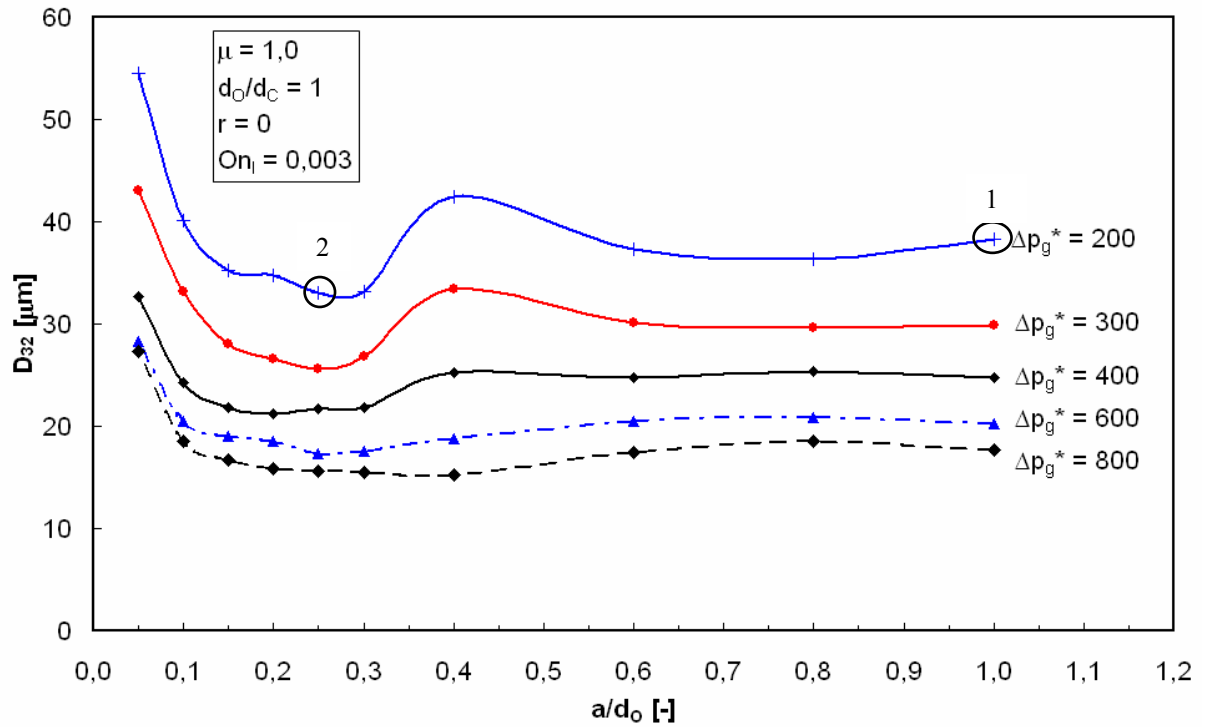


Fig. 5: Sauter mean diameter D_{32} in dependence of the related distance a/d_O at different Gas-Laplace-numbers Δp_g^* and constant liquid to air mass ratio $\mu = \dot{m}_l / \dot{m}_g = 1.0$

As illustrated in Fig. 5, the smallest D_{32} values were achieved at a distance of $a = d_0/4$. From $a = d_0/4$ on the mean drop size rises strongly with decreasing of the distance a . The influence of the distance a on the Sauter mean diameter D_{32} becomes smaller, with increasing Gas-Laplace-numbers Δp_g^* . At $\Delta p_g^* < 400$ the reduction of the distance from $a/d_0 = 0.4$ to $a/d_0 = 0.3$ results in a clear decrease of the drop size. This can be explained by the change of the disintegration regime of the liquid jet, which occurs at this point. The disintegration regimes laminar jet disintegration, aerodynamic wave jet formation and finally turbulent atomization are passed through with increasing gas pressure, respectively increasing Gas-Laplace-number Δp_g^* . During that, the Sauter mean diameter D_{32} becomes smaller with rising gas pressures at constant liquid to gas mass ratio μ . But in the case of the PEN a modification of the distance a could also result in a change of the disintegration regime. A classification of the different disintegration regimes depending on the operating condition is given in Fig. 6 for $a/d_0 = 1.0$ and Fig. 7 for $a/d_0 = 0.25$.

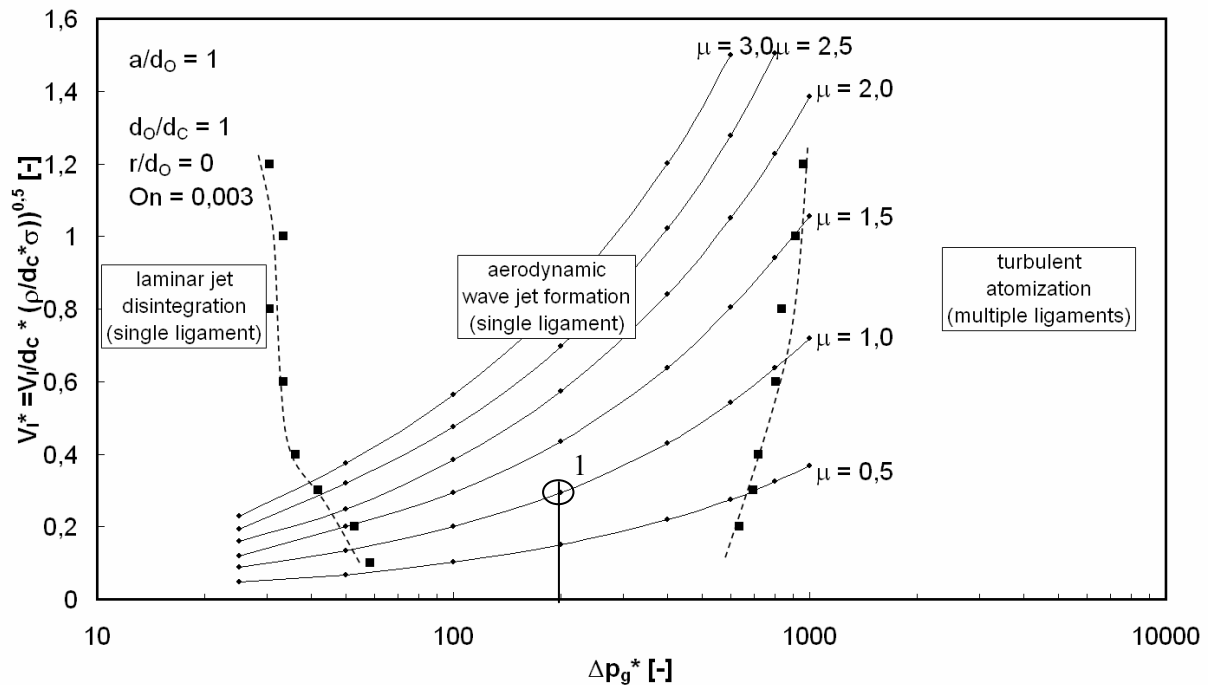


Fig. 6: Transition of the disintegration regimes in depending on Δp_g^* and \dot{V}_l^* at $a/d_0 = 1.0$

The comparison between Fig. 6 and Fig. 7 indicates that the change of the disintegration mechanism from aerodynamic wave jet formation to turbulent atomization is shifted to lower Gas-Laplace-numbers with decreasing a/d_0 . At a related distance $a/d_0 = 1.0$ and operating conditions of $\Delta p_g^* = 200$ and $\mu = 1.0$ the liquid is disintegrated by the aerodynamic wave mechanism, as illustrated in Fig. 6 (point 1). Therefore, a Sauter mean diameter $D_{32} = 42 \mu\text{m}$ was measured, as shown in Fig. 5. Reduction of the related distance from $a/d_0 = 1.0$ to $a/d_0 = 0.25$ leads to a change in the disintegration regime. Fig. 7 shows that at equal operating conditions, the liquid disintegrates by the turbulent atomization, marked with point 2. In this case the Sauter mean diameter decreases to $D_{32} = 33 \mu\text{m}$, as indicated in Fig. 5 point 2.

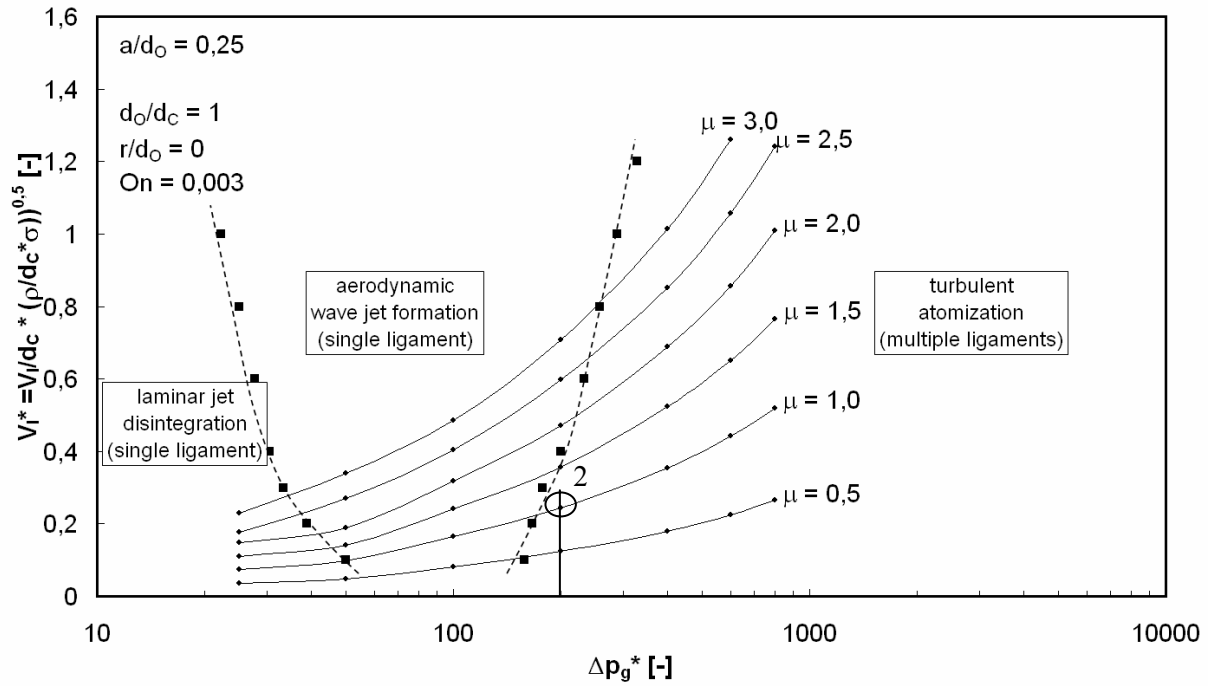


Fig. 7: Transition of the disintegration regimes in depending of Δp_g^* and \dot{V}_l^* at $a/d_o = 0.25$

Fig. 8 shows pictures of the liquid discharge from the capillary with rising gas pressures, respectively rising Gas-Laplace-numbers Δp_g^* . The pictures were made using a transparent model of the PEN with $d_c = d_o = 10$ mm and a high speed CCD-camera. The dimensionless liquid volume flux was maintained at $\dot{V}_l^* = \dot{V}_l / d_c \cdot \sqrt{\rho / (d_c \cdot \sigma)} = 0.4$. The related distance was set at $a/d_o = 1.0$ and the Ohnesorge-number was kept constant at $On = 0.0013$.

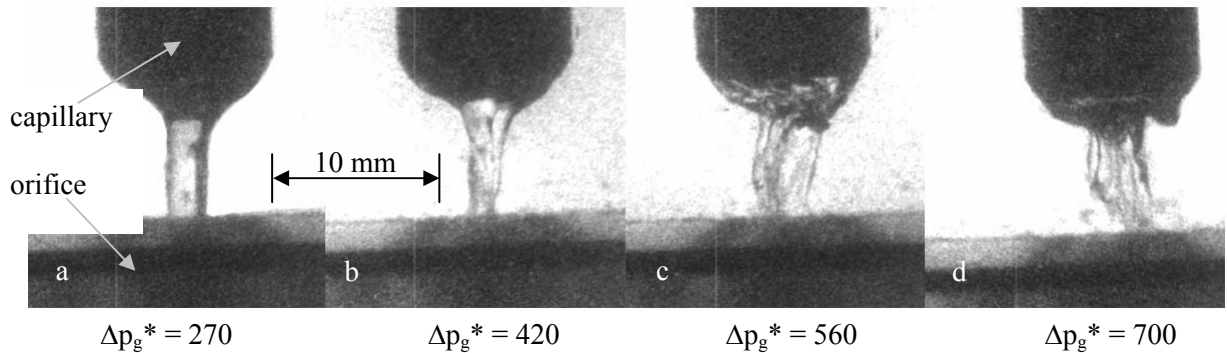


Fig. 8: Photos of liquid discharge from the capillary with increasing gas pressure, respectively increasing Gas-Laplace-number, at $\dot{V}_l^* = 0.4$, $On = 0.0013$ and $a/d_o = 1.0$

At Gas-Laplace-numbers of $\Delta p_g^* = 270$ and $\Delta p_g^* = 420$ the jet discharges from the capillary as a single ligament, Fig. 8a/b. Below the orifice, the jet disintegrates due to the aerodynamic waves. With increasing Gas-Laplace-numbers the jet becomes more turbulent. The turnover from aerodynamic wave jet formation to turbulent atomization is reached at a Gas-Laplace-number of approximately $\Delta p_g^* = 500$ at this Ohnesorge-number. At this regime, the atomization is characterised by the formation of multiple thin and irregular ligaments, as shown in Fig. 8c/d. Due to the relative fine ligaments the droplets clearly become smaller and the

break-up length becomes very short. There are no more ligaments visible below the gas orifice in case of low viscous liquids, i.e. low Ohnesorge-numbers On .

A further geometrical parameter of the PEN is the orifice inlet radius, which was still kept constant on $r = 0$ (sharp-edged) so far. A comparison of two different orifices is represented in Fig. 9.

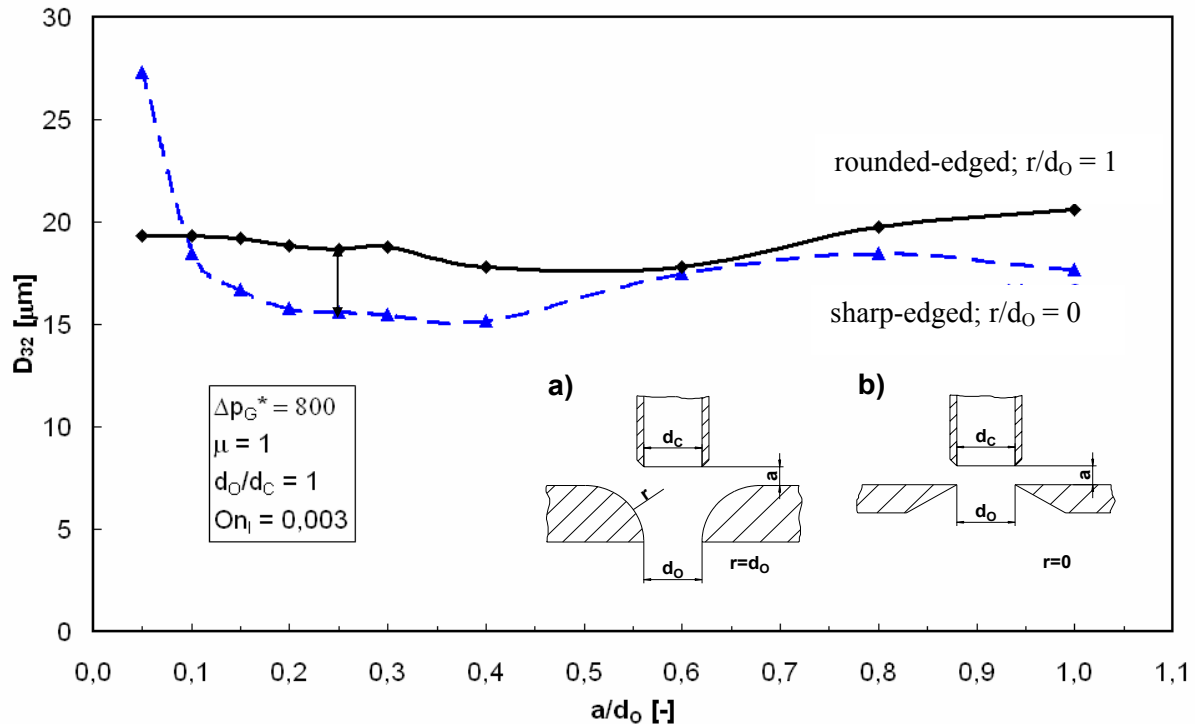


Fig. 9: Sauter mean diameter D_{32} at $\Delta p_g^* = 800$ and $\mu = 1.0$ for different orifice inlet radius r

At rounded orifice outline with $r/d_0 = 1$, the distance a has no substantial influence on the Sauter mean diameter D_{32} . At a related distance of $a/d_0 = 0.25$ the sharp-edged orifice generates a smaller Sauter mean diameters compare to the rounded orifice.

At running conditions investigated the optimum geometrical dimension for a PEN can be formed at a related distance $a/d_0 = 0.25$ with a sharp-edged orifice.

Refereces

- [1] S. Groom, H. Wiggers, P. Walzel, Sample Introduction in Atomic Emission Spectrometry (AES) Different Pneumatic Nebulizers at Comparable Operating Conditions, 18th ILASS-Conference 2002., Zaragoza (Spain), (pp. 339-344)
- [2] B.L. Sharp, *Pneumatic Nebulizers and Spray Chambers for Inductively Coupled Plasma Spectrometry*, J. Anal. At. Spectrom., **August 1988**, Vol. 3 (613-652)
- [3] A. Walz, M. Mayer, *Theoretische und experimentelle Untersuchung zur Herstellung von Stein- und Glaswolle in Blasdüsen*, Glastechnische Berichte, **Aug. 1966**, Heft 8, S. 359-370
- [4] A.M. Gañán-Calvo, A. Barrero, *A Novel Pneumatic Technique to Generate Steady Capillary Microjets*, J. Aerosol Sci., **1999**, Vol. 30 No. 1 pp. 117-125